Pilot-scale synthesis and rheological assessment of poly(methyl methacrylate) polymers: Perspectives for medical application

Lamia Zuniga Linan [a,*], Nádson M. Nascimento Lima [a], Rubens Maciel Filho [a], Marcos A. Sabino [b],
Mark T. Kozlowski [c], Flavio Manenti [d]

[a] School of Chemical Engineering, University of Campinas, UNICAMP, 13083-852 Campinas, SP, Brazil
[b] Departamento de Química, Grupo B5IDA, Universidad Simón Bolívar, 1080-A Caracas, Venezuela
[c] Division of Chemistry and Chemical Engineering, California Institute of Technology, Pasadena, CA 91125, United States
[d] Dipartamento di Chimica, Materiali e Ingegneria Chimica, Politecnico di Milano, "Giulio Natta", Piazza Leonardo da Vinci 32, 20133 Milano, Italy

Received 7 October 2014
Received in revised form 10 January 2015
Accepted 24 February 2015
Available online 25 February 2015

1. Introduction

We are currently undergoing a silent revolution. Biomaterials are proliferating, and they are used more and more frequently in clinical ap-plications to repair, rebuild, substitute for, or even regenerate damaged areas of the human body. In the United States, for instance, 38,000 vertebroplasties and 16,000 kyphoplasties using PMMA were per-formed in 2002 [1].

This has shown the need for bracing with decreasing bed rest and narcotic analgesia use. In the year 2000, the global biomaterial market was estimated at US$ 23 billion, with an annual growth rate of 12%; the estimation was surpassed in 2005 with a global market in the order of US$ 40 billion in 2005 [2,3].

Nevertheless, few countries are producing biomaterials due to their very exacting properties and specifications. For instance, Brazil imports most of its biomaterials, resulting in high costs for the Public Health Ser-vice. Because of this, Brazil has started to implement the highly scientific and technological development of biomaterials and the production of these biomaterials to meet domestic needs. It is likely that other countries face similar problems, and there is clear evidence that investigation of existing biomaterials and the development of new ones would pro-vide global benefits.

Among the most common biomaterials, the PMMA is notable for its biocompatibility. It is a widely-used polymer with many engineering applications. PMMA is a synthetic acrylic polymer, with specific proper-ties such as: natural appearance, durability, insolubility, lack of taste and odor, and low absorption in oral fluids. For these reasons, the U.S. Food and Drug Administration (FDA) approved this synthetic biomaterial for use in the fabrication of reconstructive structures [4,5].

Commercial PMMA bone cements are prepared in situ from two-component systems: the solid system, which consists of pre-polymerized PMMA, an initiator (Benzoyl Peroxide, BPO), an antibiotic (Vancomycin) and a radio-density agent (Barium Sulfate), and the liquid system, which consists mostly of the monomer Methyl Methacrylate (MMA) [6]. In situ polymerization of PMMA has a number of drawbacks, including tissue necrosis and a tendency to form membrane, as the temperature in the vicinity of the implant can increase during the polymerization, to over 100 °C [1,4,7].

Pre-fabricated implants are a viable alternative to improve the methodology of bone substitution. Espalin et al. [4] and Kim et al. [8] showed that PMMA either in filament form or in powder can be efficiently processed as scaffolds, through the Fused Deposition Modeling

* Corresponding author.
E-mail addresses: lazuli@feq.unicamp.br (L.Z. Linan), nadson@feq.unicamp.br (N.M. Nascimento Lima), maciel@feq.unicamp.br (R.M. Filho), msabino@usb.ve (M.A. Sabino), kozthought@gmail.com (M.T. Kozlowski), flavio.manenti@polimi.it (F. Manenti).

or the Powder Deposition Modeling respectively; thus, customized models can be fabricated with specific porosity and tailored mechanical properties.

An alternative we have envisioned is the fabrication of the scaffolds directly from the powder through Selective Laser Sintering (SLS) [9,10]. This method would significantly reduce the unreacted MMA monomer, the presence of which damages the local tissues. However, fabrication of PMMA powder in the laboratory, in order to satisfy strict requirements of purity, physical-chemistry properties and granulometry, is a demanding task which necessitates process control techniques and efficient purification methodologies.

Batch polymerization is widely used in industry for PMMA production because of its availability and flexibility in operation [11–14]. Nevertheless, high exothermic reactions inherent to the process require considerable effort in controller tuning to achieve proposed objectives [15]. This is because the polymerization kinetics of the MMA solution follows a free-radical mechanism. Additionally, gel-effect events are present, which generate nonlinearities and transient behavior [16].

As a result, properties, such as weight and number average molecu-lar weights, monomer conversion, polydispersity, the pore diameter and the pore volume are difficult to measure in real time. As underlined by Congalidis et al. [17], the control of these variables in a process plant is often carried out by manipulating the reaction temperature, which in-fluences them significantly.

Polymers that are formed by free-radical mechanism such as the PMMA are usually atactic and due to their random nature, atactic poly-mers are typically amorphous.

In general, physical chemistry properties of the PMMA powder used in the bone cement include: particle diameter between 1 and 125 μm; molecular weight from 60,000 to 1,000,000 g/mol; density of 1.18 g/cm^3, melting temperature of 160 °C and glass transition of 105 °C [6,18–20]. Also, the material should have high interfacial and biological compatibility and the mechanical properties of the implant should match, the mechanical properties of the tissue with which it is in contact.

Rheological properties are helpful in terms of specifications to devel-op new materials to be used in orthopedic applications. A ductile mate-rial will not be able to adequately execute their functions; similarly, if the material is much stiffer than the bone, most of the load will be trans-ferred to the implant, causing the so-called stress-shielding effect [21]. Thus, viscoelastic properties of the material should be similar to visco-elastic properties to the tissue. The rheological analysis with a parallel plate viscometer was performed with the aim to assess the viscoelastic properties of PMMA polymers to be used in medical applications. The study was focused on the measurement of viscosity, storage and loss modulus, loss factor and creep and recovery as representative measures of bone viscoelastic properties.

The polymers were synthesized in a pilot-scale laboratory plant by using an alternative combination of synthesis reagents, monomer-solvent-initiator (MMA/Ethyl acetate/AIBN), instead of the traditional Benzene and Toluene as solvent and BPO as initiator so as to reduce the toxicity of the implant, and the risk of rejection by the body.

As expected, amorphous and linear PMMA polymers were produced as a result of free-radical mechanism polymerization.

The collected results are comparable with those measured in a stan-dard PMMA polymer. Also, the increase of molecular weight improves the rheological properties, and as the molecular weight increases, the rheological properties of the polymer are getting closer those measured in human bones.

2. Experimental

2.1. Synthesis of PMMA at the pilot plant

The schematic diagram of the batch PMMA polymerization system used in this work is provided in Fig. 1. For the polymerization solution, the jacketed stainless-steel reactor with 15 l of capacity was equipped with a pitched-turbine stirrer for the mixture of the reactants. An invert-er was used to maintain the stirring speed at 360 rpm. The reactor tem-perature was controlled by manipulating both the electrical power of the thermal oil heater and the electrical power supplied to the six heating elements that act on the fluid in the jacket. The *collar type* heating elements connected in parallel to the tube of the jacket inflow varied in the range of 0.0–61.6 W to manage the reactor temperature by split-range and cascade PID control algorithm. A HP (s5520br) per-sonal computer and Programmable Logic Controller, PLC was employed for data acquisition and for monitoring and controlling the polymeriza-tion process.

The MMA was treated by using the Sigma-Aldrich prepacked column (306312) to remove the inhibitor, the ethyl acetate (99.5%, Labsynth) and the AIBN® 64 (Du-Pont) were used without additional purification. A flow rate of 0.04 l/min of gaseous nitrogen (grade 5.0 White Martins) was bubbled through the reacting medium to keep oxygen out of the re-actor. An adapted experimental procedure from Chang and Liao [13] and Ahn et al. [22] was adopted in this study. 40 ml aliquots were taken each 40 min to determine the molecular weight, the density and the viscosity. These samples were quenched with a solution of 1% w/v of Hydroquinone (CAS No. 123-31-9) in ethanol to interrupt the poly-merization and to precipitate the polymer. Details of the reactor system and specifications of the instrumentations can be found in our previous work [23,24].

Three polymers were synthesized following the process described above: two of them, at isothermal conditions of 70 °C and 60 °C, were named PMMA-70 and PMMA-60 respectively. The third one was produced by tracking a rigorous temperature trajectory in the reactor, which begins at 56 °C [24]. In this manner, a polymer with a specific mo- lecular weight was obtained, which was named PMMA-56. At the end of each polymerization, the total bulk of the reactor was properly dried and pulverized to make the rheological characterization.

A fourth polymer, the PMMA-mix consists of a mixture of 83% w/w of PMMA-56 and 17% w/w of PMMA-60, prepared from the dried powder (100 to 300 μm) of each polymer.

2.2. Physico-chemical characterization

Physico-chemical and thermo-physical properties of the polymers were measured by Size Exclusion Chromatography (SEC/GPC) and Differential Scanning Calorimetry (DSC) and compared to the properties of a reference polymer, called the PMMA-ref (182230 Aldrich, average Mw ~ 120,000 by GPC).

2.3. SEC characterization

Analysis by SEC/GPC was performed on a ViscotekGPCmax; VE2001 GPC solvent/sample module equipped with triple detector: Refractive Index (RI), Light Scattering (RALS and LALS) and on-line Viscometer. The technique leads to absolute molecular weight as well as data on solution properties. The inert, Mixed Bed ViscoGel I-Series columns: I-MBLMW-3078 and I-MBLMW-3078 (Viscotek) were used to make the measurements. For this purpose, the polymer was dissolved in tetrahydrofuran (THF) at 10 mg/ml at room temperature under soft magnetic shaking for 48 h. After that, 100 μl of each sample was filtered and automatically injected at a flow rate of 0.8 ml/min while the columns and the detector temperature were kept at 30 °C. The determination of the molecular weight distribution was based on the universal calibration technique (UNICAL), which used polystyrene, PS400K and PS65K standards (PolyCAL/Viscotek). Raw data were processed using the OmniSEC GPC/SEC Chromatography System software version 4,5,0,257. Table 1 summarizes the weight average molecular weight (M_W), the polydispersity and the Mark–Houwink exponent, α estimated by this technique.

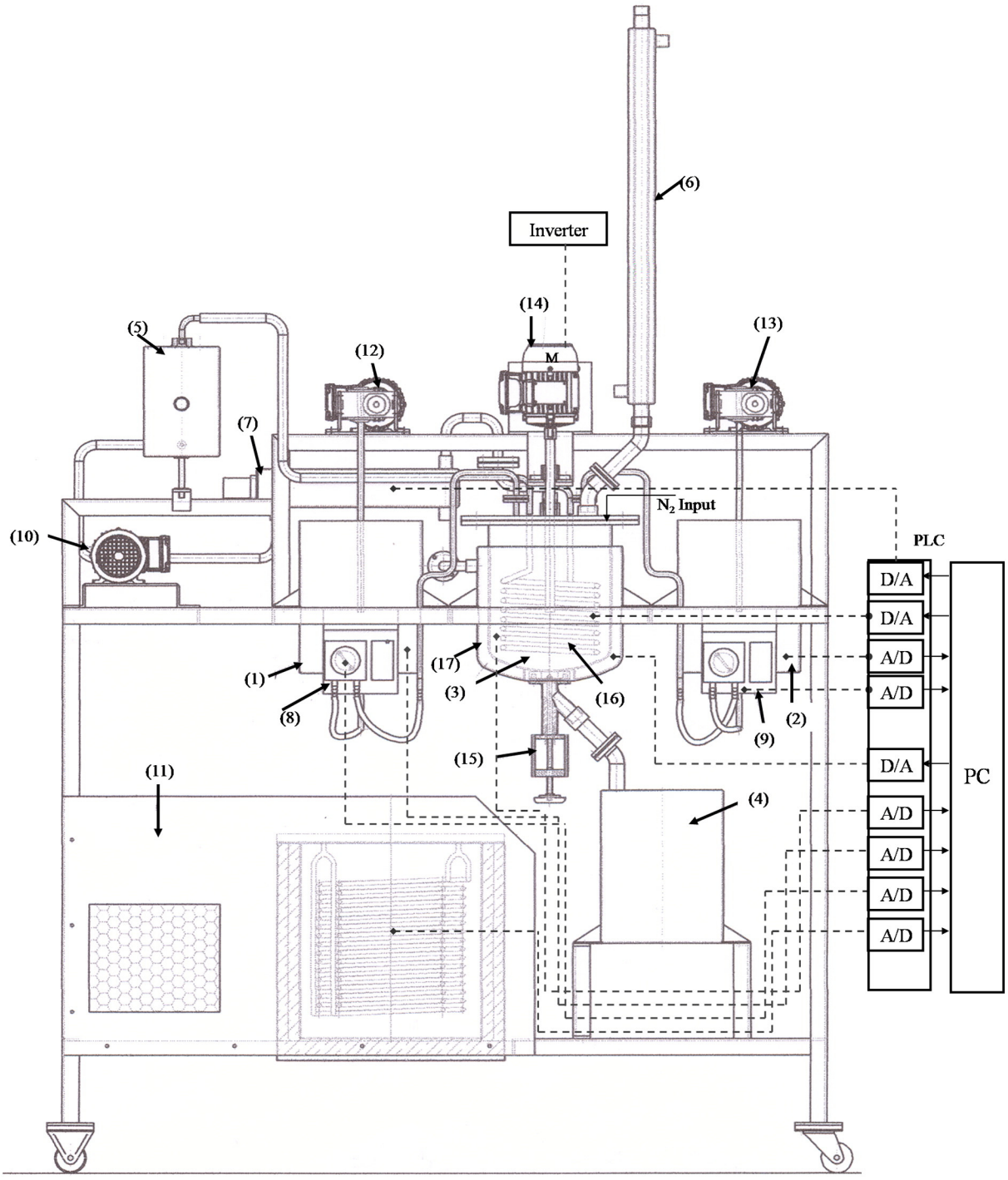

Fig. 1. Laboratory scale pilot plant with batch polymerization reactor and control unit PLC (PID) belonging to the Laboratory of Optimization, Project and Advanced Control (LOPCA)/FEQ/UNICAMP. (1) Monomer storage tank; (2) initiator and solvent storage tank; (3) BATCH polymerization reactor; (4) product storage tank; (5) thermal oil storage tank; (6) reflux condenser; (7) thermal oil heater; (8) monomer pump; (9) initiator and solvent pump; (10) thermal oil pump; (11) cooling bath; (12) monomer stirring motor; (13) initiator and solvent stirring motor; (14) reactor motor; (15) product outlet solenoid valve; (16) helical coil (serpentine); (17) jacket.

2.4. DSC characterization

DSC analysis was performed on a DSC 823e instrument (Mettler Toledo) under nitrogen atmosphere at a purge gas flow rate of 50 ml/min. Aluminum standard pans of 40 μl with hole lid were used to hold 10 mg of each sample. The scanning temperature interval was between 25 and 450 °C at a ramp rate of 10 °C/min. The glass transition, melt and degra-dation temperatures obtained from this analysis are shown in Table 1.

2.5. Treatment, handling and compression molded

The previously synthesized polymers were strictly prepared for the rheological tests. These were dried in a vacuum stove for at least one week. The drying was performed isothermally, starting at 40 °C for 96 h, followed by drying periods of 48 h at a temperature 20 °C higher. This second cycle was repeated until a final temperature of 105 °C was achieved. Thus, a total time of at least two weeks was necessary to

Table 1
Physico-chemical and thermo-physical properties of the synthesized polymers.

Property	PMMA-70	PMMA-60	PMMA-56	PMMA-ref
T_g (°C)	103	117	94	105
T_f (°C)	160	180	278	218
T-degradation (°C)	205	232	329	235
Weight-average molecular weight (Da)	44,091	86,557	213,360	120,000
Polydispersity (factor Mw/Mn)	1.507	1.685	1.543	1.469
Mark–Houwink exponent, α	0.594	0.708	0.806	0.649
Zero shear-rate viscosity at 200 °C (Pa s)	2748	21,870	367,723[a]	25,430
Steady-state recoverable compliance at 200 °C, J_e^0 (Pa^{-1}) × (10^{-3})	23.75	9.81		2.01
Steady-state recoverable compliance at 250 °C, J_e^0 (Pa^{-1}) × (10^{-3})			0.26	

[a] Estimated viscosity through the adjustment of K constant of Eq. (4).

remove a large part of the residual components of the polymers. This strict drying process was also necessary to prevent the formation of un-desirable solvent bubbles during the molding process.

As a control drying strategy, the mass of the material was measured at the end of each period; thus, the drying process finished when the polymer mass remained constant. To prevent polymerization caused by the drying temperature, a solution of 30 ppm hydroquinone in etha-nol was also added to the polymer before the start of the drying process.

After drying, the polymers were subjected to milling and pulverization, which were conducted in several stages in a M 20 Universal Mill (IKA). The cryogenic liquid nitrogen environment and the speed of 20,000 rpm reduced the particle size to nearly 100 to 300 μm, as con-firmed by a measurement on a HORIBA LA-950 laser particle size analyzer.

Finally, the powder of the polymers was compression molded into disks of 35 mm diameter and 1.0 mm thick. A work bench press composed of two pairs of rectangular plates 200 × 200 mm was used for hot and cold pressing (Labtech LP-20B). To prevent air bubbles dissolving in the disks while molding, a three-stage press methodology was established: The conditioning stage, which allows the homogenization of the polymer temperature and its relaxation from the contact to the hot plate, for 30 min; The pressurization stage, which was conducted at 145 °C and 1000 psi for 45 min, and the cooling stage at room temperature and 1000 psi for 30 min, to permit the relaxation of material before dismantling the pieces of the mold. Fig. 2 shows the disks of PMMA-56 fabricated following this methodology.

2.6. Rheological analysis

Rheological test was performed in a plate–plate PP35 with air bear-ing support sensor system (HAAKE RheoStress 6000-UTC rheometer), which measures the deflection under torque condition of the material and its regeneration when it is no longer subject to this force. All the measuring sequences were defined and controlled using RheoWin 3 *Job Manager* software.

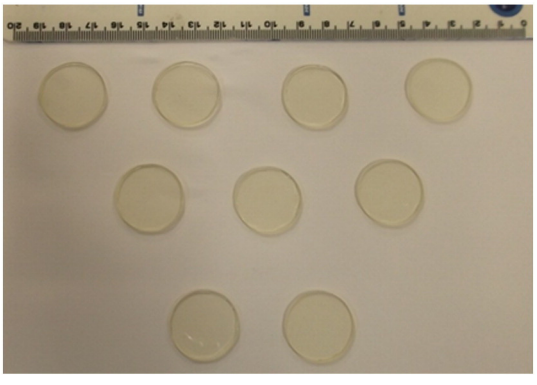

Fig. 2. Compression molded disks of PMMA-56 fabricated for rheological assessment at the rheometer.

The sensor is composed of a movable and a stationary plate with a gap of 1 mm from each other. The rheological study was carried out at two temperatures 200 °C and 250 °C, which were pre-established after a previous melting test in the sensor. Table 2 presents the experi-mental condition defined for steady state and unsteady state shear mea-surements. They include Shear Sweep, the oscillatory tests: Stress Sweep, Time Sweep, Frequency Sweep and the transient test: Creep and Recovery.

Creep–recovery experiments are sensitive methods to determine elastic properties of polymer melts [25]. In this work, Creep and Recovery tests were performed at equal times of 1500 s for each test. This time was enough to reach a stationary value for measured recoverable defor-mation. During the Creep test, a constant shear stress τ_0 is applied and the resulting time-dependent deformation $\gamma_C(t_C)$ in the linear visco-elastic range is measured. The deformation undergoes an exponential increase with the time, until a limit value, γ_∞, is achieved, thus if a tan-gent line is drawn from this point, its intersection in $t = 0$ defines the intrinsic deformation, γ_0. Next, the shear stress is to set to zero at the time t_0, and the recoverable deformation $\gamma_R(t_0, t_R)$isalsomeasured.

The creep compliance, $J_C(t_C, \tau_0)$ and the recovery compliance $J_R(t_0, t_R)$ are described by Eqs. (1) and (2), respectively:

$$J_C(t_C) = \gamma_C(t_C)/\tau_0 \tag{1}$$

$$J_R(t_0, t_R) = \gamma_R(t_0, t_R)/\tau_0. \tag{2}$$

The dependence of the deformation with the time in the linear range is represented by Eq. (3):

$$\gamma_C = \tau_0\left(J_e^0 + t/\eta\right) \tag{3}$$

where $J_e^0 = \gamma_0/\tau_0$, and J_e^0 is the steady-state linear compliance, which is a measure of the deformation during the flow and is directly influenced by the molecular weight of the polymer. On the other hand, the recovery compliance is a measure of the recoil and the elasticity of the polymer. In the linear range and for the time from t_0 to t_∞, this property is designated as the steady-state linear recovery compliance, J_e^0, which is defined as a function of γ_∞ by the relation $\gamma_\infty = \tau_0 J_e^0$.

According to Table 2, test 1 was carried out under the controlled rotation condition, while tests 2 to 5 were performed under the controlled strain condition. All the experiments were performed under a nitrogen atmosphere and for each run a new sample was used. In order to adjust the correct temperature of the samples and to reach the complete relaxing of polymer chains, a melting time of 300 s and a relaxing time between the plates of 600 s were used before starting each test.

3. Results and discussion

No crystallization events were evident during the thermal characterization by DSC, confirming the amorphous character of the PMMA.

Fig. 3a) and b) presents the viscosity profiles of the polymers in the study at 200 °C and 250 °C respectively. Pseudoplastic behavior is

Table 2
Experimental conditions established for the rheological investigations of the PMMA polymers.

Test	T/°C	Sample	τ/Pa	ω/rad s^{-1}	$\dot{\gamma}/s^{-1}$	t/s
1. Shear sweep	200	PMMA-70 PMMA-60 PMMA-ref	0.0	0.0	0.001–10.0	3480
	250	PMMA-56 PMMA-mix	0.0	0.0	0.001–10.0	1200
2. Stress sweep	200	PMMA-70 PMMA-60 PMMA-ref	1.0–1 × 10^4	1.0	0.0	837
	250	PMMA-56 PMMA-mix	1.0–1 × 10^4	1.0	0.0	837
3. Time sweep	200	PMMA-70 PMMA-60 PMMA-ref	80	6.28	0.0	4000
	250	PMMA-56 PMMA-mix	500	6.28	0.0	4000
4. Frequency sweep	200	PMMA-70 PMMA-60 PMMA-ref	80	0.0628–628.3	0.0	633
	250	PMMA-56 PMMA-mix	500	0.0628–628.3	0.00	633
5. Creep and recovery	200	PMMA-70 PMMA-60 PMMA-ref	80 (during 1500 s) 0.0 (during 1500 s)	0.0	0.0	3000
	250	PMMA-56 PMMA-mix	500 (during 1500 s) 0.0 (during 1500 s)	0.0	0.0	3000

apparent for most of the polymers, especially for the PMMA-ref (Fig. 3a) and PMMA-56 (Fig. 3b), in whose profiles three distinct regions are clearly identified: a lower Newtonian region, where the limiting vis-cosity at zero shear rate (η_0), is constant with changing shear rates, a middle region, in which the apparent viscosity (η) is decreasing, and an upper Newtonian region, where the slope of the curve (known as limiting viscosity at infinite shear rate, η_∞) is constant with changing shear rates.

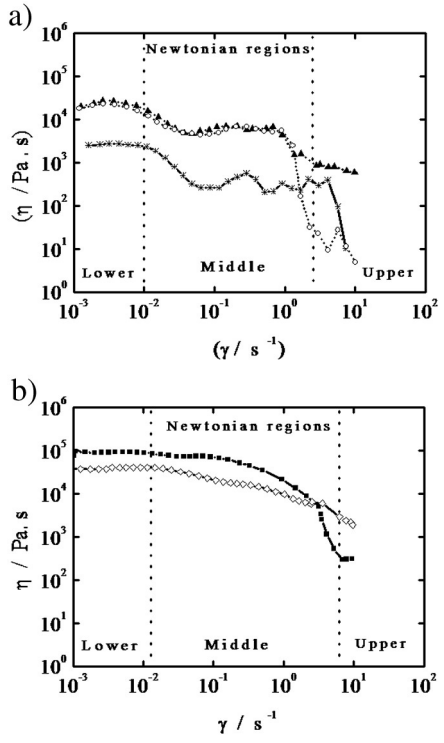

Fig. 3. Viscosity profile as a function of shear rate for polymer melts. a) At T = 200 °C: ○ PMMA-60; ▲ PMMA-ref; ✳ PMMA-70; b) at T = 250 °C: □ PMMA-56; PMMA-mix.

3.1. Steady state viscosity (zero-viscosity)

The determination of η_0 is necessary to define the relationship between the viscosity of the polymer and its molecular weight. This requires the development of a suitable model that describes the change of the viscosity as a function of the shear rate. This is because the estima-tion of the η_0 is done in an indirect manner, from the adjustment of viscosity data versus the shear rate. We found that the Carreau–Yasuda model (Eq. (4)) was able to reproduce the decreasing viscosity profiles of the polymers. Thus, the adjustment of viscosity data through the ap-plication of Eq. (4), allowed the estimation of the zero-viscosity for each sample in the shear rate range of interest (cf. Table 1). The method of Least Squares was used for this purpose.

$$\eta = \eta_\infty + (\eta_0 - \eta_\infty)\left[1 + (\lambda_1\,\dot{\gamma})^a\right]^{\frac{n-1}{a}} \quad (4)$$

where λ_1 is a time constant, a is a dimensionless parameter, and n is power law index.

In Table 3, the zero-viscosities, the model parameters, and the coefficient of determination (R^2), are recorded. As is normally adopted, for the adjustment, the parameters η_∞ and a are fixed as 0.0 and 2.0, respec-tively. It can be observed that the zero-viscosity increases with the mo-lecular weight of the polymer, thus the smallest value was found for PMMA-70 (Mw = 44,000 Da) and the largest one for PMMA-56 (Mw = 213,360 Da). In addition to the zero-viscosity, the values of the parameters λ_1 and n were adjusted in order to bring coefficient R^2

Table 3
Limiting viscosity at zero shear rate established by the Carreau–Yasuda model.

Polymer	T/°C	η_0/Pa s	λ_1	n	R^2
PMMA-70	200	2748	38.83	−1.971	0.9928
PMMA-60	200	21,870	133.3	0.08796	0.9729
PMMA-ref	200	25,460	190.3	0.5008	0.9710
PMMA-56[a]	200	367,723	–	–	–
PMMA-56	250	85,620	7.359	0.1962	0.9879
PMMA-mix	250	39,010	34.94	0.5842	0.9897

[a] Estimated viscosity through the adjustment of K constant of Eq. (4).

nearer to 1.0. As registered, the R^2 values trend to 1.0 for all the cases, therefore we consider that the estimated zero-viscosity value is reliable.

For the determination of the proportionality constant (K, in Pa s $(Da)^{-P}$) that relates the weight average molecular weight of the polymer with the zero-viscosity, an adjustment of experimental molec-ular weight data defined by SEC/GPC and the zero-viscosity, estimated by rheology is proposed. The well-known relationship of power law, Eq. (5) was used for the adjustment and two values of the slope (P index) were tested: 3.4 and 3.6 [25,26]. According to Fuchs et al. [27] and Eckstein et al. [28], for linear PMMA the viscosity–molecular weight relation (Eq. (5)) can be reliably used to determine the average molec-ular weight by measuring the limiting viscosity at zero shear rate. On the other hand, Simon and co-workers [29] reported low values of the Mark–Houwink exponent, of $\alpha = 0.395$ (measured by SEC/GPC by using a UNICAL technique) for branched PMMA and higher values, near to $\alpha = 0.688$ for linear PMMA. As can be observed in Table 1, the Mark–Houwink exponents found for the polymers of this study are rep-resentatives of the linear PMMA, thus, the properties estimated through Eq. (5) should be considered reliable.

$$\eta_0 = K(Mw)^P \tag{5}$$

Fig. 4a) and b) shows bi-logarithmic curves of the viscosity with re-spect to the average molecular weight. Three polymers PMMA-70, PMMA-60 and PMMA-ref were considered for the initial adjustment and to estimate the K values. As expected for melted homogeneous polymers, the profiles follow a straight line with slopes of 3.4 (dashed black line) and 3.6 (dashed red line). The values of K obtained for each P value are respectively $K_1 = 2.796 \times 10^{-13}$ and $K_2 = 2.946 \times 10^{-14}$. Then, K_1 and K_2 were used to calculate the zero-viscosity of PMMA-56 at 200 °C, which could not be measured by rheological analyses as the polymer was not a melt at such an experimental condition.

The viscosities $\eta_{01} = 367{,}723.49$ Pa s and $\eta_{02} = 450{,}857.76$ Pa s for $P_1 = 3.4$ and $P_2 = 3.6$ respectively are shown in Fig. 4b) as the numbers (4) and (4*) respectively.

In Fig. 4b), it is observed that the viscosity η_{01} follows the trend of previous results, thus the constant $K_1 = 2.796 \times 10^{-13}$ is chosen to rep-resent the proportionality between the viscosity and the molecular weight of PMMA-56 at 200 °C.

These results match with the work by Simon et al. [29], where a slope of P = 3.39 was observed for a linear PMMA. As a result, the vis-cosity of 367,723.49 Pa s for PMMA-56 at 200 °C is consistent with the general trend in Table 3; viscosity and molecular weight are directly correlated.

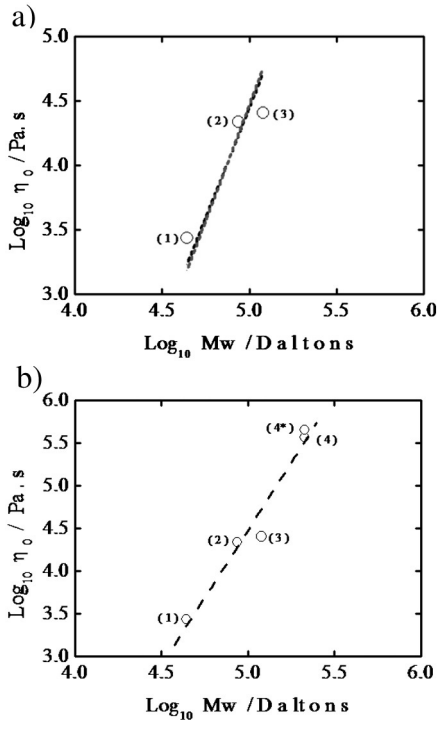

Fig. 4. Determination of proportionality constant for PMMA-56 at 200 °C of the adjustment of zero-viscosity and molecular weight of the PMMA-70, PMMA-60 and PMMA-ref polymers. a) Initial fit of experimental zero-viscosity data of (1) PMMA-70, (2) PMMA-60 and (3) PMMA-ref through Eq. (2). Dashed black and red lines are the adjustments by using $P_1 = 3.4$ and $P_2 = 3.6$ respectively; b) complete curve with zero-viscosity values for PMMA-56 at 200 °C, where (4) is the zero-viscosity value determined by using K_1 and (4*) is the value determined by using K_2.

3.2. Oscillatory test for viscoelasticity

Figs. 5 to 8 present the profile obtained from oscillatory test. Figs. 5 and 6 are the stress sweep at 200 °C for PMMA-70, PMMA-60 and PMMA-ref, and at 250 °C for the PMMA-56 and PMMA-mix respectively. The test was performed by varying the stress at a constant frequency, thus the limit of linear viscoelastic behavior is identified by means of a critical value of the sweep parameter.

The storage and loss modulus presented in Figs. 5 and 6 shows that the critical value for PMMA-60 and PMMA-ref is 10,000 Pa, above which the structural configuration of the polymers is no longer preserved. In contrast, the critical value for the PMMA-70 is 100 Pa.

For the PMMA-56 and PMMA-mix the linear viscoelastic region starts at strain values above 100 Pa and finishes at values close to 10,000 Pa.

Thus, it is worth underlining two linear viscoelastic regions where the material response has the same behavior of the applied strain. These regions are: from $1 < \tau < 100$ Pa in common for PMMA-70, PMMA-60 and PMMA-ref, and from $100 < \tau < 10{,}000$ Pa for PMMA-56 and PMMA-mix polymers. Thus, bearing in mind these results, the strains of 80 Pa and 500 Pa respectively were used to perform the rheo-logical investigation.

The thermal stability of the polymers was measured by using the time sweep test at a frequency close to the terminal region. From Figs. 7 and 8 it was shown that the storage modulus does not diverge more than 5% from its initial value at time less than 4000 s. Thus, during the rheological assessment, the structure of the materials was preserved, since the maximum evaluation time used here was 3480 s (cf. Table 2). On the other hand, according to Table 3, molecular weight did not appear to be correlated with the thermal stability of the polymers, as the profiles are constant within the 4000 s, although the storage module is different for each polymer.

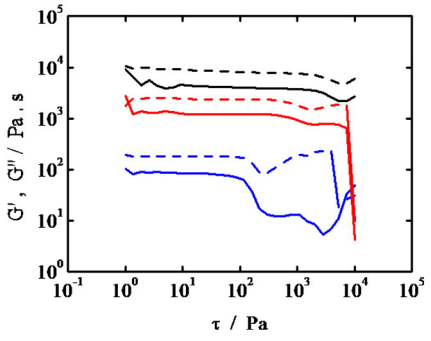

Fig. 5. Response of the PMMA polymers to the strain sweep showing the linear viscoelastic region at 1 rad s^{-1}, 200 °C under nitrogen atmosphere. ___ G′ —— G″; PMMA-ref (black line), PMMA-60 (red line), PMMA-70 (blue line). (For interpretation of the references to color in this figure legend, the reader is referred to the web version of this article.)

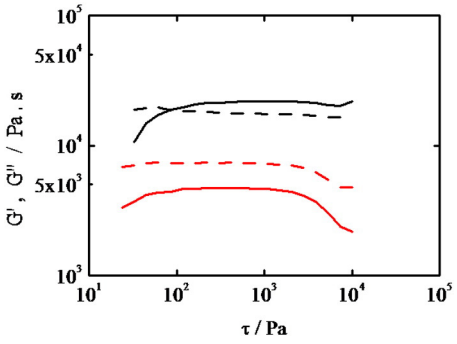

Fig. 6. Response of the PMMA polymers to the strain sweep showing the linear viscoelastic region at 1 rad s^{-1}, 250 °C under nitrogen atmosphere. ___ G′ —— G″; PMMA-56 (black line), PMMA-mix (red line). (For interpretation of the references to color in this figure legend, the reader is referred to the web version of this article.)

3.3. Transient test for viscoelasticity

Figs. 9 to 12 present the profile of storage, loss modulus, loss factor (tan δ) and complex viscosity from the frequency sweep test. Figs. 13 and 14 show the profile of creep and recoverable compliance. Several behaviors can be observed from the rheological investigation.

First of all, it is observed that the crossover frequency is influenced by the molecular weight of the polymer. Crossover occurs at high frequencies for the low molecular weight polymers (PMMA-70 and PMMA-60), and at lower frequencies for PMMA-56 and PMMA-mix, which have higher molecular weight. As expected, the crossover frequency for the PMMA-mix was between the frequency range of $1 < \omega < 10$ rad s^{-1}, which corresponds to the frequency range of its constitutive polymers (PMMA-60 and PMMA-56).

Secondly, the viscoelastic behavior of the polymers is also affected by the molecular weights. Note that the viscous behavior is prevalent ($G'' > G'$) for the smallest molecular weights, whereas the elastic behav-ior is predominant ($G' > G''$) for the largest molecular weights.

And thirdly, according to Mano [21] in dynamic mechanical analysis of viscoelastic materials, the sinusoidal response (strain) is neither ex-actly in phase with the developed stress but rather lags behind the stress by phase angle between 0° and 90°. A value of $\delta = 0°$ is typical of pure elastic material, by contrast, a value of $\delta = 90°$ is mostly present-ed in pure viscous materials. For the studied polymers, the estimated phase angles (δ) which are between $13° \leq \delta \leq 82°$, show the viscoelastic character of the material. The loss factor (tan δ) values range between 0.23 and 1.43 rad in the investigated frequency range, and as expected, this parameter is inversely dependent on polymer elasticity, then it de-creases when the storage modulus increases. In addition, a sudden in-crease of the phase angle is observed for the highest frequencies (between 10^2 and 10^3 rad s^{-1}), which is related to the increment of the loss modulus.

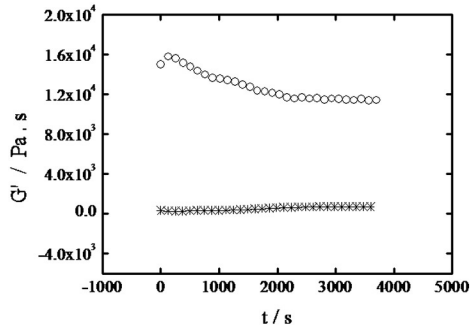

Fig. 7. Variation profile of the storage modulus as a function of the time at 200 °C, 80 Pa and 6.28 rad s^{-1} under nitrogen atmosphere. * PMMA-70; ○ PMMA-60.

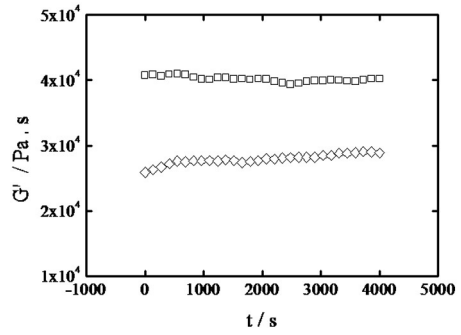

Fig. 8. Variation profile of the storage modulus as a function of the time at 250 °C, 500 Pa and 6.28 rad s^{-1} under nitrogen atmosphere. ■ PMMA-56; PMMA-mix.

Buechner and co-authors [30] showed that loss factors of the human bone vary between 0.02 and 0.04 when measured at frequencies be-tween 10^{-2} and 10^3 Hz and 0.0628 and 6.28 rad s^{-1}.

In our profiles the smallest values of this variable at the same frequency range were found for PMMA-56 (0.55 to 0.23 at frequencies

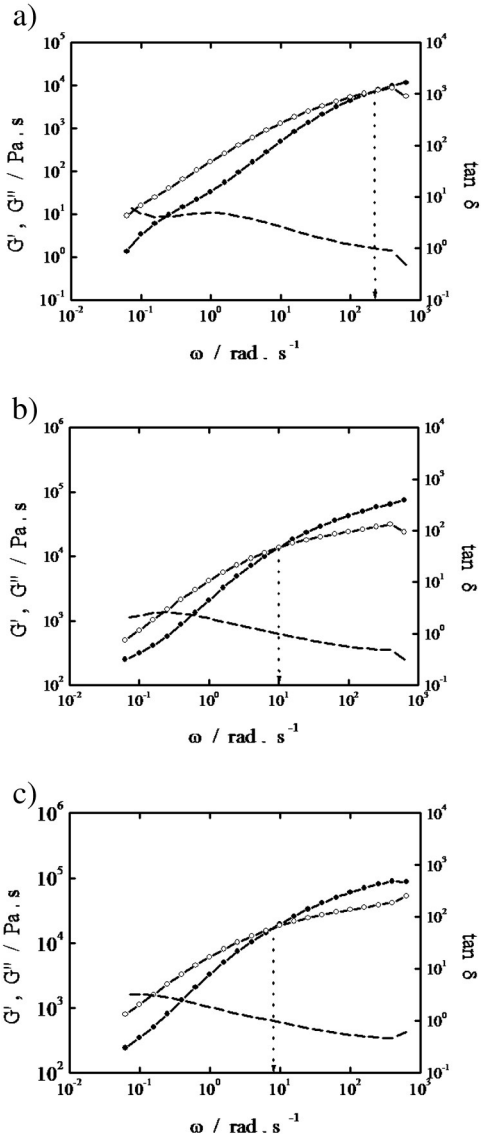

Fig. 9. Profiles of storage modulus (G′), loss modulus (G″) and loss factor with frequency (ω) at 80 Pa, 200 °C under nitrogen atmosphere for a) PMMA-70, b) PMMA-60 and c) PMMA-ref. ● and ○ are G′ and G″ values respectively; scatter line is the tan δ.

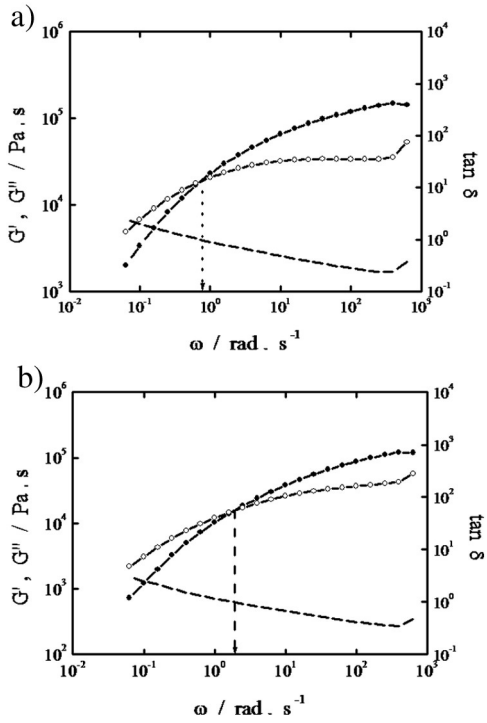

Fig. 10. Profiles of storage modulus (G′), loss modulus (G″) and loss factor with frequency (ω) at 500 Pa, 250 °C under nitrogen atmosphere for a) PMMA-56 and b) PMMA-mix. ● and ○ are G′ and G″ values respectively; scatter line is the tan δ.

between 6.28 and 396 rad s^{-1} respectively), which has the highest molecular weight. What it is strongly important to highlight is, even though the polymers synthesized in this work still do not have the suitable properties to be used in the orthopedic field (since their behavior is more viscous than elastic), it is possible to envisage that better characteristics of the material can be obtained for polymers with higher molecular weight, as the loss factor decreases when the molecular weight increases. According to the established methodology of synthesis and previous simulations, higher molecular weights can be obtained at polymerization temperatures lower than 56 °C.

The complex viscosity showed a uniform decrease with the increase of the frequency. The influence of the molecular weight was a distinct feature in the results, as higher viscosities were obtained for the polymers with higher molecular weight.

According to the Creep–recovery tests, all materials showed typical behavior of viscoelastic polymers, as when the load was applied, an instantaneous elastic response was observed, followed by a delayed reaction after the removal of the strain.

PMMA-70 showed a high viscosity as a consequence of its low molecular weight as well as the lowest percentage recovery, 0.20%

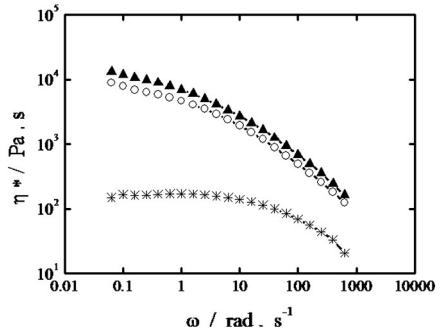

Fig. 11. Profile of complex viscosity with frequency (ω) at 80 Pa, 200 °C under nitrogen atmosphere. ▲ PMMA-ref; * PMMA-70; ○ PMMA-60.

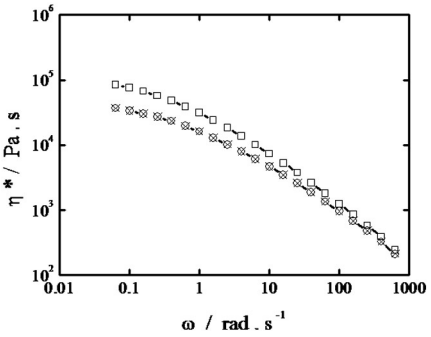

Fig. 12. Profile of complex viscosity with frequency (ω) at 500 Pa, 250 °C under nitrogen atmosphere. □ PMMA-56; ⊗ PMMA-mix.

compared to PMMA-60 and PMMA-ref, which have a recovery of 10.5% and 17.3% respectively.

The results for PMMA-56 and PMMA-mix at 250 °C were respectively 7.25% and 2.0%. Note that the elasticity of these polymers increases as the molecular weight, and this property influences the recovery of the material. Conversely, a proportional relationship between the steady-state shear compliance, J_e^0, the molecular weight, and the polydispersity of the polymer is not identified.

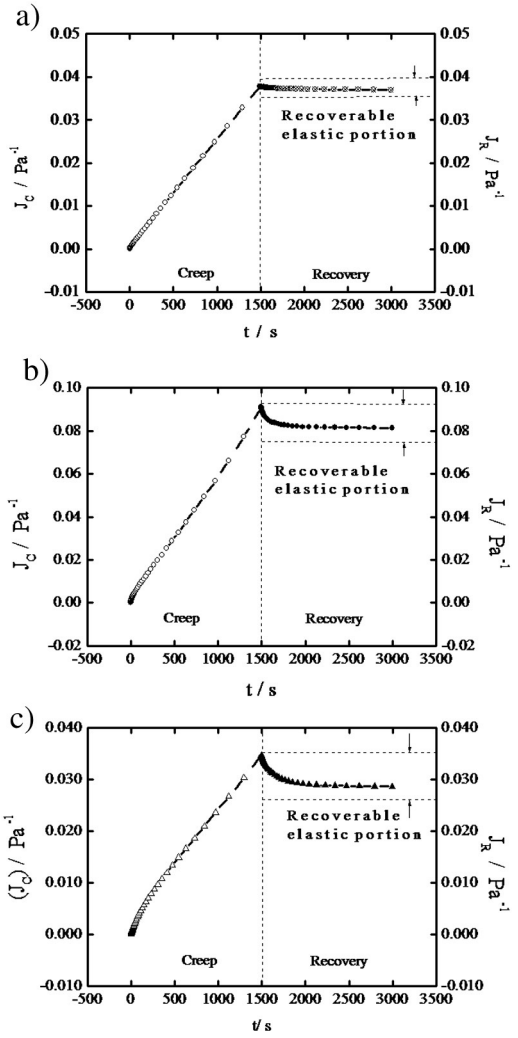

Fig. 13. Creep–recovery profiles at 80 Pa, 200 °C under nitrogen atmosphere. a) PMMA-70; b) PMMA-60; c) PMMA-ref.

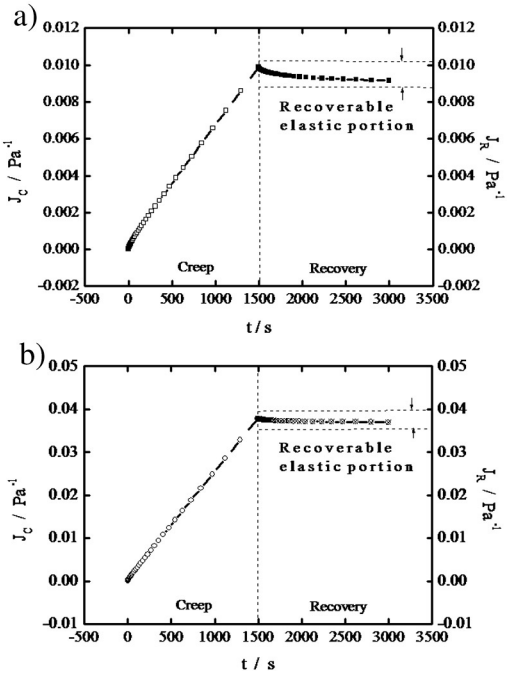

Fig. 14. Creep–recovery profiles at 500 Pa, 250 °C under nitrogen atmosphere. a) PMMA-56; b) PMMA-mix.

In Table 1 the highest value of this property obtained for the PMMA-70 is in disagreement with the one defined for the PMMA-60 and the PMMA-ref. The polymer might therefore demonstrate Rouse behavior in this case.

According to Fuchs et al. [27] and Fetters et al. [31], polymers of PMMA with small molecular weight exhibit Rouse behavior in the pro-file of steady-state shear compliance, J_e^0 versus molecular weight. This behavior is described by a steep-slope straight line in the first part of the curve, which represents high values of J_e^0 at low molecular weight. This trend is typical in PMMA whose molecular weight is approaching the critical molar mass. On the other hand, for polymers with molecular weight much greater than the critical molar mass, a plateau behavior is observed. The values of J_e^0 for the polymers PMMA-60 and PMMA-ref tend to this plateau, which is justified because of their higher molecular weights.

4. Concluding remarks

As a first stage toward scaffold fabrication a synthesis methodology of PMMA in a pilot-scale laboratory plant was implemented. The polymers were synthesized according to the specific directives and matching the final properties of biomaterial production.

The polymer showed an increase of their molecular weight as the initial reaction temperature in the batch reactor was decreasing. The results of the characterization analysis showed that properties such as viscosity, storage and loss modulus of the synthesized polymers were comparable to those measured in a commercial polymer considered as reference.

Rheological analysis showed that the molecular weight of the polymers influences their viscoelastic behavior. Therefore, the highest molecular weight polymers showed the predominance of elasticity, whereas polymers characterized by the smallest molecular weight showed the highest viscosity.

From the loss factor profiles and from the comparison with literature data, it was possible to highlight that the properties of the PMMA approach those of human bone properties as the molecular weight increases, at least within the frequency interval investigated in this study.

Additionally, from chromatographic and rheological analysis it was possible to estimate the proportionality constant between the viscosity and the molecular weight of the polymer at 200 °C. The value of this constant is comparable with the one indicated in the literature for traditional polymers.

Solution properties (Mark–Houwink exponent) from the SEC/GPC confirmed that the synthesized polymers have linear structure, and are atactic and amorphous.

The PMMA polymers produced with the proposed methodology were satisfactory and presented improved characteristics if compared to the commercial polymers and from the perspective of managing in optimal manner the most sensitive variables of the process, it will be possible to obtain ideal polymers for the medical purposes in the next future.

Finally, tests of toxicity in-vitro and in-vivo, conducted in cells (NCTC clone 929/ATCC) and rats (Heterogeneous/WISTAR) (to be presented in a separate publication), showed continuous and progressive growing of the cells on the surface and around the implanted PMMA samples. Thus, the synthesized and handled polymers following the early described methodology do not present toxicity risk and can be used for our proposed medical applications.

Acknowledgments

This work was supported by the São Paulo State Research Support Foundation/Fundação de Amparo à Pesquisa do Estado de São Paulo (FAPESP), Grant numbers 2008/57860-3, 2009/09092-0, 2011/09631-8, and 2010/16952-2 and by the National Counsel of Technological and Scientific Development (CNPq)/INCT-BIOFABRIS/FEQ/UNICAMP, Grant number 573661/2008-1.

References

[1] R.Q. Frazer, R.T. Byron, P.B. Osborne, K.P. West, PMMA: an essential material in med-icine and dentistry, J. Long-Term Eff. Med. Implants 15 (2005) 629–639.
[2] V.J. Dalosto, Sintese e caracterização do Poli (L - ácido láctico) para uso como bioma-terial, Departamento de Engenharia de Materiais, Escola de Engenharia. Universidade Federal do Rio Grande do Sul, Porto Alegre, 2005. (79 p. These (In Por-tuguese). Retrieved from:<http://www.lume.ufrgs.br/bitstream/handle/10183/ 6945/000492758.pdf?…1>. Accessed in Sep 30 2014).
[3] S.G. De Almeida, Biomateriais. Forum de biotecnologia de materiais(In Portuguese) http://www.redetec.org.br/publique/media/tr10_biomateriais.pdf2005 (Accessed in May 05 2013, Retrieved from:).
[4] D. Espalin, K. Arcaute, D. Rodriguez, F. Medina, Fused deposition modeling of patient-specific polymethylmethacrylate implants, Rapid Prototyp. J. 16 (2010) 164–173.
[5] J.D. Kretlow, M. Shi, S. Young, P.P. Spicer, N. Demian, J.A. Jansen, M.E. Wong, F.K. Kasper, A. Mikos, Evaluation of soft tissue coverage over porous polymethylmethacrylate space maintainers within nonhealing alveolar bone defects, Tissue Eng. Part C Methods 16 (2010) 1427–1438.
[6] J.G.F. Santos, L.S. Peixoto, M. Nele, P.A. Melo, J.C. Pinto, Theoretical and experimental investigation of the production of PMMA-based bone cement, Macromol. Symp. 243 (2006) 1–12.
[7] M. Stańczyk, Study on modelling of PMMA bone cement polymerization, J. Biomech. 38 (2005) 1397–1403.
[8] B. Kim, K. Hong, K. Park, D. Park, Y. Chung, S. Kang, Customized cranioplasty implants using three-dimensional printers and polymethyl-methacrylate casting, J. Korean Neurosurg. Soc. 52 (2012) 541–546.
[9] L. Liulan, H. Qingxi, H. Xianxu, X. Gaochun, Design and fabrication of bone tissue en-gineering scaffolds via rapid prototyping and CAD, J. Rare Earths 25 (2007) 379–383.
[10] G.V. Salmoria, J.L. Leite, C.N. Lopes, R.A.F. Machado, A. Lago, The manufacturing of PMMA/OS blends by selective laser sintering, in: P.J. Bartolo, et al., (Eds.), Virtual and Rapid Manufacturing, Taylor & Francis Group, London, 2008, pp. 305–311.
[11] J. Chang, J. Lai, Computation of optimal temperature policy for molecular weight control in a batch polymerization reactor, Ind. Eng. Chem. Res. 31 (1992) 861–868.
[12] H. Rho, Y. Huh, H. Rhee, Application of adaptive model-predictive control to a batch MMA polymerization reactor, Chem. Eng. Sci. 53 (1998) 3729–3739.
[13] J. Chang, P. Liao, Molecular weight control of a batch polymerization reactor: exper-imental study, Ind. Eng. Chem. Res. 38 (1999) 144–153.
[14] E. Pahija, F. Manenti, I.M. Mujtaba, Selecting the best control methodology to improve the efficiency of discontinuous reactors, in: A. Kraslawski, I. Turunen (Eds.), Computer Aided Chemical Engineering, Elsevier, Amsterdam, 2013, pp. 805–810.
[15] N.M.N. Lima, L.L. Zuniga, R. Maciel Filho, M.R. Wolf Maciel, M. Embiruçu, F. Grácio, Modeling and predictive control using fuzzy logic: application for a polymerization system, AICHE J. 56 (2010) 965–978.

[16] A.J.B. Antunes, J.A.F.R. Pereira, A.M.F. Fileti, Fuzzy control of a PMMA batch reactor: development and experimental testing, Comput. Chem. Eng. 30 (2005) 268–276.
[17] J.P. Congalidis, J.R. Richards, W.H. Ray, Feedforward and feedback control of a solu-tion copolymerization reactor, AICHE J. 35 (1989) 891–907.
[18] R. Mendes, Estudo experimental comparativo dos cimentos ósseos nacionais, http://www.maxwell.lambda.ele.puc-rio.br/9823/9823_3.PDF2006 (Accessed in Septem-ber 23 2014., M.Sc. Tese (In Portuguese). Retrieved from).
[19] W.F. Mousa, M. Kobayashi, S. Shinzato, M. Kamimura, M. Neo, S. Yoshihara, T. Nakamura, Biological and mechanical properties of PMMA-based bioactive bone ce-ments, Biomaterials 21 (2000) 2137–2146.
[20] M.L. Bruens, H. Pieterman, J.R. de Winjn, J.M. Vaandrager, Porous polymethylmethacrylate as bone substitute in the craniofacial area, J. Craniofac. Surg. 14 (2003) 63–68.
[21] J.F. Mano, Viscoelastic properties of bone: mechanical spectroscopy studies on a chicken model, Mater. Sci. Eng. C 25 (2005) 145–152.
[22] S. Ahn, S. Chang, H. Rhee, Application of optimal temperature trajectory to batch PMMA polymerization reactor, J. Appl. Polym. Sci. 69 (1998) 59–68.
[23] L.L. Zuniga, N.M.N. Lima, L.P. Tovar, F. Manenti, R. Maciel Filho, M.R. Wolf Maciel, M. Embiruçu, Pilot-plant simulation, experimental campaign and rigorous modeling of a batch MMA polymerization reactor for the fabrication of bone tissue, in: I.D. Lockhart, M. Fairweather (Eds.), Computer Aided Chemical Engineering, Elsevier, Amsterdam, 2012, pp. 1352–1356.
[24] N.M.N. Lima, L.L. Zuniga, F. Manenti, R. Maciel Filho, M.R. Wolf Maciel, M. Embiruçu, Novel two-steps optimal control of batch polymerization reactors and application to PMMA production for the fabrication of artificial bone tissue, in: A. Kraslawski, I. Turunen (Eds.), Computer Aided Chemical Engineering, Elsevier, Amsterdam, 2013, pp. 163–168.
[25] H. Muenstedt, K. Nikolaos, J. Kaschta, Rheological properties of poly(methyl methac-rylate)/nanoclay composites as investigated by creep recovery in shear, Macromol-ecules 41 (2008) 9777–9783.
[26] W.H. Tuminello, Molecular weight and molecular weight distribution from dynamic measurements of polymer melts, Polym. Eng. Sci. 26 (1986) 1339–1347.
[27] K. Fuchs, C. Friedrich, J. Weese, Viscoelastic properties of narrow-distribution poly(methylmethacrylate), Macromolecules 29 (1996) 5893–5901.
[28] A. Eckstein, J. Suhm, C. Friedrich, R.D. Maier, J. Sassmannshausen, M. Bochmann, R. Mülhaupt, Determination of plateau moduli and entanglement molecular weights of isotactic, syndiotactic, and atactic polypropylenes synthesized with metallocene catalysts, Macromolecules 31 (1998) 1335–1340.
[29] P.F. Simon, A.H.E. Müller, T. Pakula, Characterization of highly branched poly(methyl methacrylate) by solution viscosity and viscoelastic spectroscopy, Macromolecules 34 (2001) 1677–1684.
[30] P.M. Buechner, R.S. Lakes, C.S. Swan, R.A. Brand, A broadband viscoelastic spectro-scopic study of bovine bone: implications for fluid flow, Ann. Biomed. Eng. 29 (2001) 719–728.
[31] L.J. Fetters, D.J. Lohse, S.T. Milner, W.W. Graessley, Packing length influence in linear polymer melts on the entanglement, critical, and reputation molecular weights, Macromolecules 32 (1999) 6847–6851.